Wave-turbulence theory of four-wave nonlinear interactions

Sergio Chibbaro, Giovanni Dematteis, Christophe Josserand, Lamberto Rondoni

PHYSICAL REVIEW E **96**, 021101(R) (2017)

Wave-turbulence theory of four-wave nonlinear interactions

Sergio Chibbaro,[1] Giovanni Dematteis,[2,*] Christophe Josserand,[1,3] and Lamberto Rondoni[2,4,5]

[1]*Sorbonne Université, UPMC Université Paris 06, CNRS, UMR 7190, Institut Jean Le Rond d'Alembert, F-75005 Paris, France*

[2]*Dipartimento di Scienze Matematiche, Politecnico di Torino, Corso Duca degli Abruzzi 24, I-10129 Torino, Italy*

[3]*Laboratoire d'Hydrodynamique (LadHyX), UMR 7646 CNRS-Ecole Polytechnique, F-91128 Palaiseau Cedex, France*

[4]*INFN, Sezione di Torino, Via P. Giuria 1, I-10125 Torino, Italy*

[5]*MICEMS, Universiti Putra Malaysia, 43400 Serdang Selangor, Malaysia*

(Received 9 February 2017; published 30 August 2017)

The Sagdeev-Zaslavski (SZ) equation for wave turbulence is analytically derived, both in terms of a generating function and of a multipoint probability density function (PDF), for weakly interacting waves with initial random phases. When the initial amplitudes are also random, a one-point PDF equation is derived. Such analytical calculations remarkably agree with results obtained in totally different fashions. Numerical investigations of the two-dimensional nonlinear Schrödinger equation (NLSE) and of a vibrating plate prove the following: (i) Generic Hamiltonian four-wave systems rapidly attain a random distribution of phases independently of the slower dynamics of the amplitudes, vindicating the hypothesis of initially random phases. (ii) Relaxation of the Fourier amplitudes to the predicted stationary distribution (exponential) happens on a faster time scale than relaxation of the spectrum (Rayleigh-Jeans distribution). (iii) The PDF equation correctly describes dynamics under different forcings: The NLSE has an exponential PDF corresponding to a quasi-Gaussian solution, as the vibrating plates, that also shows some intermittency at very strong forcings.

DOI: 10.1103/PhysRevE.96.021101

Introduction. Dispersive waves are ubiquitous in nature, and their nonlinear interactions make them intriguing and challenging [1,2]. Wave turbulence is the theory that describes the statistical properties of large numbers of incoherent interacting waves, with tools such as the wave kinetic equation, analytically derived in the late 1960's. This equation describes the evolution of the wave spectrum in time, when homogeneity and weak nonlinearity are assumed [3–5]. It has been applied to numerous phenomena, including ocean waves [6–8], capillary waves [9,10], Alfvén waves [11], optical waves [12], and solid oscillations [13–18]. It is the analog of the Boltzmann equation for classical particles and it allows the Rayleigh-Jeans equilibrium state as well as nonequilibrium solutions, in terms of Kolmogorov-Zakharov (KZ) spectra [19].

To characterize the invariant measure of the dynamics, that is, to find the complete statistical description concerning all quantities of interest, an important step has been taken by Sagdeev and Zaslavski [20], who obtained the Brout-Prigogine equation for the probability density function (PDF) of wave turbulence [21]. More recently, this statistical framework has been nicely revisited using the diagrammatic technique [4] and performing analytical calculations, in the three-wave case [22–24]. Interestingly, many experimental and theoretical results have shown that deviations from wave-turbulence predictions can be found for rare events, e.g., intermittency [8,25–29]. This seems to be the case when a more general theoretical framework [30–34] is required, because the nonlinearities are not small [35,36].

In this Rapid Communication, a complete wave-turbulence theory is developed for a fully general four-wave system, whose Hamiltonian is expressed by the following canonical expression,

$$H = \frac{1}{2}\sum_{1} \omega_1 A_1^{\sigma_1} A_1^{-\sigma_1} + \epsilon \sum_{1234} \mathcal{H}^{\sigma}_{\underline{\mathbf{k}}}\, A_1^{\sigma_1} A_2^{\sigma_2} A_3^{\sigma_3} A_4^{\sigma_4}\, \delta_{\underline{\sigma}\cdot\underline{\mathbf{k}},\mathbf{0}}. \quad (1)$$

Here, ω_1 is the normal frequency of wave 1, which nonlinearly interacts with waves 2, 3, and 4 with a coupling constant $\mathcal{H}^{\sigma}_{\underline{\mathbf{k}}}$, $\sum_i \doteq \sum_{\sigma_i=\pm1}\sum_{\mathbf{k}_i\in\Lambda_L^*}$, $\Lambda_L^* = \frac{2\pi}{L}\mathbb{Z}^d_M$. $A^{\sigma}_{\mathbf{k}} = \frac{1}{\sqrt{2}}(P_{\mathbf{k}} + i\sigma Q_{\mathbf{k}})$ are the canonical variables of the wave field, whose real and imaginary parts are the coordinates and momenta. $\sigma = \pm 1$ represents the "spin" of a wave, so that $A^{+}_{\mathbf{k}} \doteq A_{\mathbf{k}}$, $A^{-}_{\mathbf{k}} \doteq A^*_{\mathbf{k}}$ (* is the complex conjugation).

Theory. Given the Hamiltonian (1), we concisely derive the equations of motion in terms of canonical normal variables; the details are given in Ref. [37]. First, recall that the action-angle variables (amplitudes and phases) for the linear dynamics are defined by $J_{\mathbf{k}} = |A^{\sigma}_{\mathbf{k}}|^2$ and $\varphi_{\mathbf{k}} = \sigma \arg(A^{\sigma}_{\mathbf{k}})$, so that $A^{\sigma}_{\mathbf{k}} = \sqrt{J_{\mathbf{k}}}\psi^{\sigma}_{\mathbf{k}}$, where $\psi_{\mathbf{k}} = \exp(i\varphi_{\mathbf{k}})$. Then, the Liouville measure μ preserved by the Hamiltonian flow reads $d\mu = \prod_{\mathbf{k}} dQ_{\mathbf{k}} dP_{\mathbf{k}} = \prod_{\mathbf{k}} \frac{1}{i} dA^{+}_{\mathbf{k}} dA^{-}_{\mathbf{k}} = \prod_{\mathbf{k}} \frac{1}{i} da^{+}_{\mathbf{k}} da^{-}_{\mathbf{k}} = \prod_{\mathbf{k}} dJ_{\mathbf{k}} d\varphi_{\mathbf{k}}$. $A^{\sigma}_{\mathbf{k}}$ and $a^{\sigma}_{\mathbf{k}}$ are linked by the rotation in the complex plane, $A^{\sigma}_{\mathbf{k}} = a^{\sigma}_{\mathbf{k}} e^{i\sigma\omega_{\mathbf{k}}t}$. The equations of motion with four-wave interactions can thus be expressed by ($\sigma = +1$ when it is omitted)

$$\begin{aligned}\frac{\partial a_1}{\partial t} = \epsilon \sum_{234} & \mathcal{L}^{+\sigma_2\sigma_3\sigma_4}_{1234} a_2^{\sigma_2} a_3^{\sigma_3} a_4^{\sigma_4} \\ & \times \exp\left[i(-\omega_1 + \sigma_2\omega_2 + \sigma_3\omega_3 + \sigma_4\omega_4)t\right] \\ & \times \delta_{-\mathbf{k}_1+\sigma_2\mathbf{k}_2+\sigma_3\mathbf{k}_3+\sigma_4\mathbf{k}_4,\mathbf{0}}. \end{aligned} \quad (2)$$

For a system with N modes in a box of size L, the complete statistical description of the field is given by the generating function, defined by

$$\mathcal{Z}_L[\lambda,\mu,T] \doteq \left\langle \exp\left(\sum_{\mathbf{k}\in\Lambda_L^*} \lambda_{\mathbf{k}} J_{\mathbf{k}}(T)\right) \prod_{\mathbf{k}\in\Lambda_L^*} \psi^{\mu_{\mathbf{k}}}_{\mathbf{k}}(T) \right\rangle, \quad (3)$$

where $\lambda_{\mathbf{k}} \in \mathbb{R}$, $\mu_{\mathbf{k}} \in \mathbb{Z}$, $\forall \mathbf{k} \in \Lambda_L^*$.

*Corresponding author: giovannidematteis@gmail.com

Assuming that the canonical wave field enjoys a random phase (RP) property at the initial time, we have averaged over phases using the Feynman-Wyld diagrams [4]. Further, taking the large-box limit, we have normalized the amplitudes in such a way that the wave spectrum remains finite. This step is crucial for the evaluation of the different diagrams [24]. Then, taking the large-box limit, followed by the small nonlinearity limit, and introducing the nonlinear time $\tau = \epsilon^2 T$, we have formally obtained the following closed equation for the generating function (the characteristic functional),

$$\frac{d\mathcal{Z}[\lambda,\mu,\tau]}{d\tau} = -192\pi\delta_{\mu,0} \times \sum_{\underline{\sigma}} \int d^d k_1 d^d k_2 d^d k_3 d^d k_4 \lambda(\mathbf{k}_1) \left|\mathcal{H}_{1234}^{-\sigma_2\sigma_3\sigma_4}\right|^2 \delta\left(\tilde{\omega}_{234}^1\right) \times \delta_{234}^1 \left(\frac{\delta^3\mathcal{Z}}{\delta\lambda(\mathbf{k}_2)\delta\lambda(\mathbf{k}_3)\delta\lambda(\mathbf{k}_4)} - \sigma_2 \frac{\delta^3\mathcal{Z}}{\delta\lambda(\mathbf{k}_1)\delta\lambda(\mathbf{k}_3)\delta\lambda(\mathbf{k}_4)} - \sigma_3 \frac{\delta^3\mathcal{Z}}{\delta\lambda(\mathbf{k}_1)\delta\lambda(\mathbf{k}_2)\delta\lambda(\mathbf{k}_4)} - \sigma_4 \frac{\delta^3\mathcal{Z}}{\delta\lambda(\mathbf{k}_1)\delta\lambda(\mathbf{k}_2)\delta\lambda(\mathbf{k}_3)} \right), \quad (4)$$

which constitutes the main ingredient of the present Rapid Communication. The frequency in $\delta(\tilde{\omega}_{234}^1)$ has been renormalized [4] as $\tilde{\omega}_{\mathbf{k}} \doteq \omega_{\mathbf{k}} + \Omega_{\mathbf{k}}$, taking into account the self-interactions possible in four-wave systems that do not contribute to the nonlinear interactions but shift the linear frequency.

The characteristic functional constitutes the most detailed description of the phenomenon [38], for which the following holds: (i) The RP property of the initial field is preserved in time, implying the validity of Eq. (4) for $\tau > 0$. (ii) Equation (4) has a solution preserving in time the stricter random phase and amplitude (RPA) property of an initial wave field, i.e., the possible factorization of $\mathcal{Z}[\lambda,\mu,0]$. (iii) Differentiating with respect to the $\lambda_{\mathbf{k}}$'s, the spectral hierarchy for the moments, analogous to the Bogoliubov-Born-Green-Kirkwood-Yvon (BBGKY) hierarchy in kinetic theory, is obtained. Then, RPA allows us to close the hierarchy, leading to the wave spectrum equation, the kinetic equation.

As the characteristic functional gives information that is too detailed, in relevant situations we have derived the equation for the characteristic function $\mathcal{Z}^{(M)}$, which concerns a number M of modes, and enjoys the same properties of $\mathcal{Z}[\lambda,\mu,\tau]$ [37]. Then, under the RPA hypothesis, we derived a closed fully general equation for the one-mode PDF that reads [37]

$$\frac{\partial P}{\partial \tau} = -\frac{\partial F}{\partial s} = \frac{\partial}{\partial s}\left[s\left(\eta_{\mathbf{k}} \frac{\partial P}{\partial s} + \gamma_{\mathbf{k}} P \right) \right], \quad (5)$$

$$\eta_{\mathbf{k}} \doteq 192\pi \sum_{\underline{\sigma}} \int d^d\mathbf{k}_2 d^d\mathbf{k}_3 d^d\mathbf{k}_4 \delta_{234}^{\mathbf{k}} \delta\left(\tilde{\omega}_{234}^{\mathbf{k}}\right) \left|\mathcal{H}_{\mathbf{k}234}^{-\sigma_2\sigma_3\sigma_4}\right|^2 \times n(\mathbf{k}_2)n(\mathbf{k}_3)n(\mathbf{k}_4) \geqslant 0,$$

$$\gamma_{\mathbf{k}} \doteq 192\pi \sum_{\underline{\sigma}} \int d^d\mathbf{k}_2 d^d\mathbf{k}_3 d^d\mathbf{k}_4 \delta_{234}^{\mathbf{k}} \delta\left(\tilde{\omega}_{234}^{\mathbf{k}}\right) \left|\mathcal{H}_{\mathbf{k}234}^{-\sigma_2\sigma_3\sigma_4}\right|^2 \times [\sigma_2 n(\mathbf{k}_3)n(\mathbf{k}_4) + \sigma_3 n(\mathbf{k}_2)n(\mathbf{k}_3) + \sigma_4 n(\mathbf{k}_2)n(\mathbf{k}_3)]. \quad (6)$$

The conservation equation for P explicitly expresses F, the flux of the one-mode probability in the amplitude space. This is a nonlinear Markov evolution equation in the sense of McKean. As a matter of fact, the solutions must satisfy a set of self-consistency conditions $n(\mathbf{k},\tau) = \int ds\, s P(s,\tau;\mathbf{k})$, where $n(\mathbf{k},\tau)$ is the spectrum that also appears in the formulas for the coefficients (6). The derivation of the standard kinetic equation from Eq. (5) is straightforward. Let us assume that the wave-turbulence picture is valid for $s \in (0, s_{\mathrm{nl}})$, where the upper bound of the interval can also be $+\infty$ (a fact that will be discussed later). Using (5), the definition of the wave spectrum $n(\mathbf{k}) = \int_0^{s_{\mathrm{nl}}} s P(s) ds$ and integrating by parts, we obtain

$$\frac{\partial n}{\partial \tau} = \eta_{\mathbf{k}} - \gamma_{\mathbf{k}} n - s_{\mathrm{nl}}(F(s_{\mathrm{nl}}) + \eta_{\mathbf{k}} P(s_{\mathrm{nl}})). \quad (7)$$

The last term is a null term that has to vanish in order for the equation to be satisfied in general, giving a boundary condition in the amplitude space at $s = s_{\mathrm{nl}}$. What we are left with is simply the kinetic equation. To make it clear for a concrete example of a four-wave resonant system where not only two waves $\rightarrow$ two waves interactions are present, we derive the kinetic equation for the vibrating plates [13]. Writing (7) in the two-dimensional case, we obtain

$$\frac{\partial n}{\partial \tau} = 192\pi \sum_{\underline{\sigma}} \int d^2\mathbf{k}_1 d^2\mathbf{k}_2 d^2\mathbf{k}_3 \delta_{123}^{(2)\mathbf{k}} \delta\left(\tilde{\omega}_{123}^{\mathbf{k}}\right) \left|\mathcal{H}_{\mathbf{k}\mathbf{k}_1\mathbf{k}_2\mathbf{k}_3}^{-\sigma_2\sigma_3\sigma_4}\right|^2 \times n_{\mathbf{k}} n_1 n_2 n_3 \left(\frac{1}{n_{\mathbf{k}}} + \frac{\sigma_1}{n_1} + \frac{\sigma_2}{n_2} + \frac{\sigma_3}{n_3} \right), \quad (8)$$

which is the same equation as in Refs. [13,39]: The quantity $J_{-\mathbf{k}\mathbf{k}_1\mathbf{k}_2\mathbf{k}_3}$ in Ref. [13] corresponds to $4i\mathcal{H}_{\mathbf{k}\mathbf{k}_1\mathbf{k}_2\mathbf{k}_3}^{-\sigma_2\sigma_3\sigma_4}$ because of the way their coefficients relate to the Hamiltonian coefficients. Therefore, a factor of 16 appears, making the two equations identical. The equation for the PDF can be written also as the following set of stochastic differential equations,

$$ds_{\mathbf{k}} = (\eta_{\mathbf{k}} - \gamma_{\mathbf{k}} s_{\mathbf{k}}) d\tau + \sqrt{2\eta_{\mathbf{k}} s_{\mathbf{k}}}\, dW_{\mathbf{k}}, \quad (9)$$

interpreted in the Itô sense and with the self-consistent determination of $n(\mathbf{k},\tau)$. An important solution of (5) is the distribution

$$Q(s,\tau;\mathbf{k}) = \frac{1}{n(\mathbf{k},\tau)} e^{-s/n(\mathbf{k},\tau)}. \quad (10)$$

In the absence of forcing and dissipation, an H theorem and the law of large numbers for the empirical spectrum imply that the solution relaxes to Q, for typical initial wave fields [24,37]. It strictly describes thermodynamic equilibrium only when n is stationary, but our results show (see Fig. 1) that P tends to the asymptotic state Q before n has reached its stationary state. This justifies that Q be called the distribution of equilibrium despite its formal dependence on time. Furthermore, the results in Fig. 2 suggest that relaxation to equilibrium also extends to forced and damped systems.

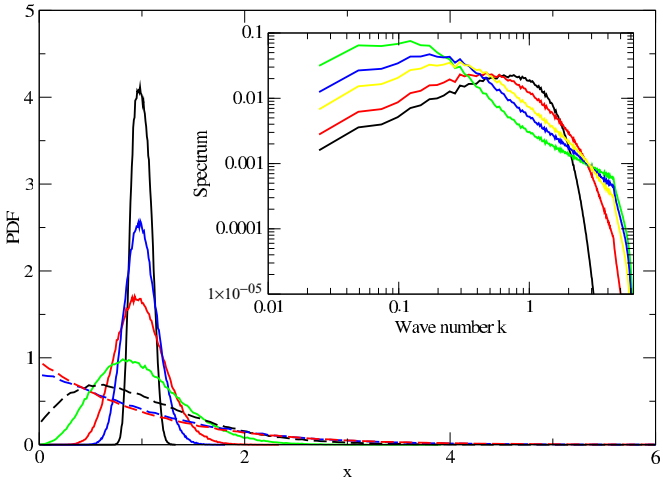

FIG. 1. Normalized PDFs of the modes $|\Psi_{\mathbf{k}}(\tau)|^2$ for $|\mathbf{k}| = 2$ as a function of the normalized quantity $x = |\Psi_k(\tau)|^2/n(k,\tau)$, where $n(k,\tau)$ is the mean value of $|\Psi_k(\tau)|^2$. The numerical simulation of the 2D NLSE is performed over a domain of size 256×256 using a regular square grid of mesh size $dx = 0.5$ so that 512×512 modes are simulated. The statistics and mean values are obtained both by an ensemble average over 128 realizations of the numerical simulation of the NLS equation starting at $\tau = 0$ with a Gaussian Fourier mode distribution with random phases, and using the isotropy of the fields allowing an angular mean. The PDFs are shown for $\tau = 0.01$, 0.03, 0.05, 0.1, 0.2, 0.5, and 1 time units, respectively, from top to bottom. The short-time PDFs are concentrated around the mean value while they converge at a large time to the expected e^{-x} law (corresponding to the dashed red line, PDF for $\tau = 10$) and no more variations of the PDFs are observed for $\tau > 10$. The inset shows the spectrum $n(k,\tau)$ for the times $\tau = 0.1$, 10, 30, 50, and 110, from bottom to top, respectively, looking at low k. The equipartition of energy spectrum $n(k,\tau) \propto 1/k^2$ is still not reached for the latest time shown here.

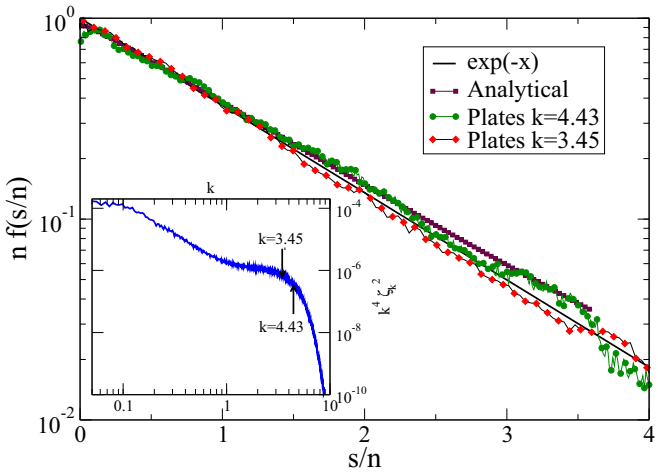

FIG. 2. Normalized PDFs of the Fourier modes $|\zeta_k|^2$ as a function of the rescaled parameter s/n for two different wave numbers $k = 3.45$ and $k = 4.43$, in a linear-log plot. The statistical average is made using an angle average due to the isotropy of the system and time average, because of the statistically stationary regime reached in time. Here, $dx = 0.25$ and the square plate is $L \times L = 1024 \times 1024$, meaning that 4096×4096 modes are simulated. The PDFs are reasonably well fitted by the equilibrium law e^{-x}, although for $k = 4.43$ the generalized function (11) with the cutoff $s_{\rm nl} = 3.6n(k)$ is a much better fit. The inset shows the compensated spectrum $k^4|\zeta_k|^2$ that exhibits a complex inertial regime, with a k^{-2} slope at large scale ($k \lesssim 1$), indicating intermittent behavior, and the expected weak-turbulence spectrum $|\zeta_k|^2 \propto k^{-4}$ at smaller scales ($1 < k < 5$), where the two modes shown here are located [35]. The other modes' PDFs show, outside of the forcing region ($k < 0.05$), the exponential Rayleigh distribution.

The general stationary solution to Eq. (5) reads [4,22]

$$P(s) = Ce^{-s/\nu} - \frac{F_*}{\eta_{\mathbf{k}}}\,\mathrm{Ei}\left(\frac{s}{\nu}\right)e^{-s/\nu}, \tag{11}$$

where $\mathrm{Ei}(x)$ is the integral exponential function $\mathrm{Ei}(x) = -\int_{-x}^{\infty}\frac{e^{-t}}{t}dt$. Equation (11) is obtained by enforcing a constant probability flux in amplitude space, $F(s) = -s(\eta_{\mathbf{k}}\frac{\partial P}{\partial s} + \gamma_{\mathbf{k}}P) \equiv F_*$. For the positivity of $P(s)$ for $s \gg \nu$, F_* must be negative, corresponding to a probability flux from the large to small amplitudes. This must be physically motivated by the existence of strong nonlinear interactions (e.g., breaking of wave crests) which feed probability into the weak, near-Gaussian background. In this picture, this happens at $s = s_{\rm nl}$, and due to the strong nonlinear effects, $P(s)$ decays very quickly for $s > s_{\rm nl}$. Thus, the cutoff amplitude $s_{\rm nl}$ and the stationary flux F_* are two aspects of the same phenomenon, connected to each other through the boundary condition that comes out of (7) in a natural way,

$$P(s_{\rm nl}) = -F_*/\eta_{\mathbf{k}}. \tag{12}$$

This is consistent with the fact that if the weak-turbulence assumption holds over the whole amplitude space, $s \in (0,\infty)$, the normalization of probability implies $F_* = 0$, and the equilibrium exponential distribution is recovered, as expected in the absence of strong nonlinear effects that would affect the dynamics. So, clearly the picture with the cutoff is meant to describe systems where forcing and damping are present at some wave numbers, which are necessary to sustain strong nonlinear phenomena. Then, the corrective term in (11) represents the increased probability in the tail of the distribution due to such nonlinear phenomena [$\mathrm{Ei}(x) \propto \frac{1}{x}$ for $x \gg 1$].

Before numerically verifying this scenario, some remarks are in order. At variance with previous studies [22,24], we do not need a probability sink to allow the solution, because we have $F(s) = F_*$ for $s \in (0,s_{\rm nl})$ (similarly as in Ref. [4]). Integrating (5) from 0 to $s_{\rm nl}$, $\frac{\partial}{\partial t}\int_0^{s_{\rm nl}} ds\,P(s) = F(s = s_{\rm nl}) - F(s = 0) = 0$, it is seen that the normalization of the probability in the system is preserved. This appears natural when considering the logarithmic variable $\sigma = \ln(s)$, whose probability density $\Pi(\sigma)$ satisfies

$$\partial_t \Pi = -\partial_\sigma F, \tag{13}$$

with the same F of Eq. (5). Imposing $F(s = 0) = F_*$, as in the rest of the interval, just means that there is a probability flux from $\sigma_{\rm nl} = \ln(s_{\rm nl})$ toward $\sigma = -\infty$, with probability transferred to infinitesimally small amplitudes. In the stationary

state, using (12) and normalizing the probability yields

$$C = \frac{1}{\nu}\left(1 + \frac{\Gamma + \ln\frac{s_{\rm nl}}{\nu} - e^{-\frac{s_{\rm nl}}{\nu}}\,\mathrm{Ei}\left(\frac{s_{\rm nl}}{\nu}\right)}{e^{\frac{s_{\rm nl}}{\nu}} - \mathrm{Ei}\left(\frac{s_{\rm nl}}{\nu}\right)}\right)^{-1}, \qquad (14)$$

where $\Gamma \simeq 0.5772$ is the Euler-Mascheroni constant, and $P(s) = \frac{1}{\nu}e^{-s/\nu}$, in the $s_{\rm nl} \to \infty$ limit. As $s_{\rm nl}$ becomes finite, the complete solution has to be chosen (with $F_* < 0$) and this contribution brings a correction to the asymptotic solution. In conclusion, given the cutoff value $s_{\rm nl}$, which enters as a parameter of the model, and the spectrum $\nu = \eta/\gamma$ in the equilibrium limit, the two free constants in (11) are fixed and a unique general solution with a cutoff is obtained.

Numerical results. In order to validate these analytical predictions, we performed numerical simulations for two prototype equations of four-wave turbulence. The first is the nonlinear Schrödinger equation (NLSE) in two dimensions, modeling, for instance, the propagation of electromagnetic fields in optic fibers [40],

$$i\partial_t \Psi = -\tfrac{1}{2}\Delta\Psi + |\Psi|^2\Psi, \qquad (15)$$

where $\Delta = \partial_x^2 + \partial_y^2$ is the Laplacian operator and Ψ is a field taking complex values. The second is the Föppl–von Kármán (FvK) equation in two space dimensions for the vibrations of elastic plates [41], which in dimensionless form reads

$$\frac{\partial^2\zeta}{\partial t^2} = -\tfrac{1}{4}\Delta^2\zeta + \{\zeta,\chi\}, \qquad (16)$$

$$\Delta^2\chi = -\tfrac{1}{2}\{\zeta,\zeta\}. \qquad (17)$$

χ is the Airy stress function imposing the compatibility condition for the displacement field and the Poisson bracket $\{\cdot,\cdot\}$ is defined by $\{f,g\} \equiv f_{xx}g_{yy} + f_{yy}g_{xx} - 2f_{xy}g_{xy}$, so that $\{\zeta,\zeta\}$ is the Gaussian curvature.

The reason for investigating these two models is that they exhibit an important difference in four-wave interactions: While the NLSE only allows a two waves $\to$ two waves collision kernel, because of an additional conservation law, the FvK equation allows one wave $\to$ three waves collisions as well. Both equations are solved in a periodic square domain using similar numerical schemes involving a pseudospectral method (see, for instance, Ref. [13] for details on the numerical methods). We first investigate the evolution of the fields starting with a Gaussian distribution [consisting for NLSE of $|\psi(\mathbf{k},0)|^2 \propto e^{-k^2/k_0^2}$ with a random phase]: The initial PDF of the amplitudes is given by $P(x) = \delta(x-1)$ for each mode, where $x = s/n(0)$ is the normalized amplitude. The evolution of the one-mode PDF is shown in Fig. 1, together with the time evolution of the density spectrum (inset). We can see that $P(x)$ converges rapidly to the exponential solution given by Eq. (10), in agreement with the theory. Interestingly, the dynamics of the spectrum is different. The spectrum converges towards the equilibrium solution given by the Rayleigh-Jeans spectrum [3], but the characteristic time is much larger: The PDF has reached equilibrium when the spectrum is still far from it. That validates the theory and, in particular, it supports the RPA approximation, which appears to be verified from whatever initial conditions after extremely short times. The same dynamics was also observed for the elastic plate (not shown here). This evidence confirms the results already obtained for a general three-wave system [42].

Then, we study the nonequilibrium wave-turbulence energy cascade for the elastic plate dynamics obtained by injecting energy at large scale through a random noise in Fourier space at small k and a dissipation dominant at small scale. The balance between these two contributions leads to a stationary regime with a wave-turbulence spectrum following roughly $|\zeta_k|^2 \sim k^{-4}$ at low forcing (up to a logarithmic correction [13]) that corresponds to a constant flux of energy from the large to the small scales. It is thus tempting to compare the PDF of the Fourier modes of this dynamics with that of the Hamiltonian dynamics studied above, for which the theory has been derived. Indeed, no theoretical predictions can be easily made in such a configuration, because the forcing-dissipation terms break the Hamiltonian structure. Moreover, while a distribution close to the one of the equilibrium situation could be expected at low forcing, intermittency at high forcing is supposed to heavily influence the PDF of the Fourier mode, similarly to what has been observed for the high moments of the structure function in real space [35]. Surprisingly, Fig. 2 shows that the PDFs are very close to the Rayleigh distribution predicted for the Hamiltonian dynamics, in the absence of flux ($F_* = 0$) even at high forcing where the spectrum exhibits a k^{-6} slope at small k. However, a closer analysis shows a slight deviation from this distribution for modes at small scales, just before the dissipative range, where the PDF is better fitted by the generalized distribution (11) with $F_* \neq 0$. Similar results have also been observed for the NLSE with no noticeable nonzero F_*. The weak value of F_* obtained for our systems suggests that while a clear signature of intermittency is detected in physical space via structure functions [35], it is difficult to find anomalous scaling looking at the one-mode spectral PDF. On one hand, the effect is expected to be small for those systems where the spectrum of wave turbulence is only a small logarithmic correction to the equilibrium spectrum, so that the dominant signal in the fluctuations of the spectrum is due to the statistical equilibrium contribution. This is certainly the case for NLSE. On the other hand, Fig. 2 suggests a nontrivial interplay between large and small scales, since in vibrating plates the spectrum is definitely far from equipartition at large scales, but the signature of intermittency is found at very small scales, even in physical space [35]. This issue deserves future investigation.

Acknowledgment. The authors gratefully acknowledge the referee's insightful remarks that also allowed them to correct one error.

[1] G. B. Whitham, *Linear and Nonlinear Waves* (Wiley, Hoboken, NJ, 2011), Vol. 42.

[2] M. Berry, Nature (London) **403**, 21 (2000).

[3] G. Falkovich, V. Lvov, and V. Zakharov, *Kolmogorov Spectra of Turbulence* (Springer, Berlin, 1992).

[4] S. Nazarenko, *Wave Turbulence*, Lecture Notes in Physics Vol. 825 (Springer, Berlin, 2011).

[5] A. C. Newell and B. Rumpf, Annu. Rev. Fluid Mech. **43**, 59 (2011).
[6] G. Komen, L. Cavaleri, M. Donelan, K. Hasselmann, H. Hasselmann, and P. Janssen, *Dynamics and Modeling of Ocean Waves* (Cambridge University Press, Cambridge, UK, 1994).
[7] M. Onorato, A. R. Osborne, M. Serio, D. Resio, A. Pushkarev, V. Zakharov, and C. Brandini, Phys. Rev. Lett. **89**, 144501 (2002).
[8] E. Falcon, S. Fauve, and C. Laroche, Phys. Rev. Lett. **98**, 154501 (2007).
[9] A. N. Pushkarev and V. E. Zakharov, Phys. Rev. Lett. **76**, 3320 (1996).
[10] C. Falcon, E. Falcon, U. Bortolozzo, and S. Fauve, Europhys. Lett. **86**, 14002 (2009).
[11] S. Galtier, S. Nazarenko, A. C. Newell, and A. Pouquet, J. Plasma Phys. **63**, 447 (2000).
[12] A. Picozzi, J. Garnier, T. Hansson, P. Suret, S. Randoux, G. Millot, and D. Christodoulides, Phys. Rep. **542**, 1 (2014).
[13] G. Düring, C. Josserand, and S. Rica, Phys. Rev. Lett. **97**, 025503 (2006).
[14] N. Mordant, Phys. Rev. Lett. **100**, 234505 (2008).
[15] A. Boudaoud, O. Cadot, B. Odille, and C. Touzé, Phys. Rev. Lett. **100**, 234504 (2008).
[16] B. Miquel, A. Alexakis, C. Josserand, and N. Mordant, Phys. Rev. Lett. **111**, 054302 (2013).
[17] T. Humbert, O. Cadot, G. Düring, C. Josserand, S. Rica, and C. Touzé, Europhys. Lett. **102**, 30002 (2013).
[18] T. Humbert, C. Josserand, C. Touzé, and O. Cadot, Physica D **316**, 34 (2016).
[19] V. Zakharov and N. Filonenko, Sov. Phys. Dokl. **11**, 881 (1967).
[20] G. Zaslavskii and R. Sagdeev, Sov. Phys. JETP **25**, 718 (1967).
[21] R. Brout and I. Prigogine, Physica **22**, 621 (1956).
[22] Y. Choi, Y. V. Lvov, S. Nazarenko, and B. Pokorni, Phys. Lett. A **339**, 361 (2005).
[23] Y. Choi, Y. V. Lvov, and S. Nazarenko, Physica D **201**, 121 (2005).
[24] G. L. Eyink and Y.-K. Shi, Physica D **241**, 1487 (2012).
[25] A. Majda, D. McLaughlin, and E. Tabak, J. Nonlinear Sci. **7**, 9 (1997).
[26] E. Falcon, S. Aumaître, C. Falcón, C. Laroche, and S. Fauve, Phys. Rev. Lett. **100**, 064503 (2008).
[27] S. Lukaschuk, S. Nazarenko, S. McLelland, and P. Denissenko, Phys. Rev. Lett. **103**, 044501 (2009).
[28] S. Nazarenko, S. Lukaschuk, S. McLelland, and P. Denissenko, J. Fluid Mech. **642**, 395 (2009).
[29] E. Falcon, S. Roux, and C. Laroche, Europhys. Lett. **90**, 34005 (2010).
[30] A. C. Newell, S. Nazarenko, and L. Biven, Physica D **152**, 520 (2001).
[31] L. Biven, S. Nazarenko, and A. Newell, Phys. Lett. A **280**, 28 (2001).
[32] C. Connaughton, S. Nazarenko, and A. Newell, Physica D **184**, 86 (2003).
[33] Y. V. Lvov and S. Nazarenko, Phys. Rev. E **69**, 066608 (2004).
[34] P. Jakobsen and A. C. Newell, J. Stat. Mech. (2004) L10002.
[35] S. Chibbaro and C. Josserand, Phys. Rev. E **94**, 011101 (2016).
[36] S. Chibbaro, F. De Lillo, and M. Onorato, Phys. Rev. Fluids **2**, 052603 (2017).
[37] S. Chibbaro, G. Dematteis, and L. Rondoni, arXiv:1611.08030.
[38] A. Monin and A. Yaglom, *Statistical Fluid Mechanics: Mechanics of Turbulence* (Dover, New York, 2007).
[39] G. Düring, C. Josserand, and S. Rica, Physica D **347**, 42 (2017).
[40] S. Dyachenko, A. Newell, A. Pushkarev, and V. Zakharov, Physica D **57**, 96 (1992).
[41] L. Landau and E. Lifshitz, *Theory of Elasticity* (Pergamon Press, New York, 1959).
[42] M. Tanaka and N. Yokoyama, Phys. Rev. E **87**, 062922 (2013).